

Switching probability investigation of electric field-induced precessional magnetization switching

Hongguang Cheng and Ning Deng

Institute of Microelectronics, Tsinghua University, Beijing 100084, P. R. China

E-mail: chenghg7932@gmail.com

Abstract

We report theoretical investigation of the switching probability of electric field-induced precessional magnetization switching by solving the Fokker-Planck equation numerically with finite difference method. The switching probability is determined by the net magnetic field induced by the deviation of precession angle from its equilibrium position after precession process. The error rate has the lowest value under an appropriate applied external field for the voltage pulse duration τ_{pulse} a little longer than the half precession period. The calculated results show that ultra-low error rate down to the order of 10^{-12} can be achieved for thermal stability factor $\Delta = 50$ and low damping factor material should be used for free layer to improve the switching probability. For parallel (anti-parallel) magnetization to anti-parallel (parallel) magnetization switching process, the spin transfer torque tends to decrease (increase) the error rate when the τ_{pulse} is shorter than the half precession period, and increase (decrease) the error rate when τ_{pulse} is longer than the half-period. These results exhibit potential of electric field-induced precessional magnetization switching for ultra-low power, high speed magnetic random access memory (MRAM) application.

1. Introduction

Electric field-induced precessional magnetization switching utilizing the interfacial voltage-controlled magnetic anisotropy [1-12] to modify the free layer perpendicular anisotropy field has been demonstrated recently [13-16]. A bistable magnetization switching with sub-nanosecond switching time is realized by applying a unipolar voltage pulse in FeCo/MgO/Fe magnetic tunnel junction [13, 15]. Its realization in CoFeB/MgO materials system [14, 16] is of most technological importance for the capability of high density integration with conventional semiconductor industry and large tunnel magnetoresistance ratio [17, 18]. Magnetization reversal induced by electric field only consumes charging and discharging energy, it can reduce writing power consumption by more than two orders of magnitude compared with the spin transfer torque (STT) induced switching. Therefore, electric field-induced precessional magnetization switching is a promising candidate for ultra-low power and high speed magnetic random access memory (MRAM) applications.

Due to the thermal fluctuations of magnetization direction, switching error may take place in the switching process. The switching probability is defined by the number of error-free switching events divided by the number of total switching events. It characterizes the reliability of device write operation. Error rate is one minus switching probability. Ultra-low error rate should be achieved for high-reliability applications. In STT induced switching, the error rate can be unlimited close to zero by increasing the write duration time. While in electric field-induced precessional magnetization switching, the error rate is a limited value. The order of error rate can be achieved and the factors influence the switching probability need to be made clear. In previous studies [13-16] the switching probability is obtained qualitatively by repeating macro-spin model simulation or micro-magnetic simulation hundreds of times. This could not be used to investigate the switching events with ultra-low error rate quantitatively. Although the error rate can be obtained by experimental approach [19, 20], theoretical investigation of error rate quantitatively is necessary to design the electric field-induced precessional magnetization switching device.

In this paper, we report quantitative calculations of the switching probability of electric field-induced precessional magnetization switching with in-plane easy axis [13, 15] by solving the Fokker-Planck equation [21] numerically with finite difference method based on

macro-spin model. We investigated the mechanism that switching errors take place and discussed the influence of thermal stability factor, damping factor of free layer and spin transfer torque effect on the switching probability.

2. Model and methods

Figure 1 demonstrates the schematic geometry of the electric field-induced precessional magnetization switching. θ and φ are the direction angles describing the orientation of the macro-spin moment \mathbf{M} of free layer in spherical coordinates. The in-plane coercive field \mathbf{H}_c is parallel to the x axis. The external magnetic field \mathbf{H}_{ext} is applied along the positive direction of z axis. The calculated trajectories by macro-spin model simulation based on zero temperature Landau-Lifshitz-Gilbert (LLG) equation are shown in figure 1(a)-(b). $\mathbf{M}_{initial}$ and \mathbf{M}_{final} denote the initial and final magnetization state before and after voltage pulse duration τ_{pulse} . The blue line represents the precession process during τ_{pulse} , and the red line represents the relaxation process after τ_{pulse} .

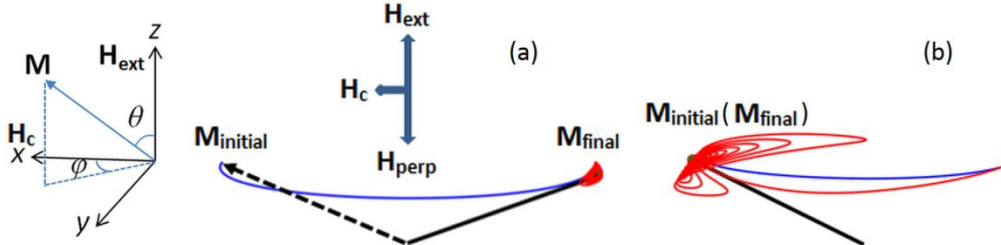


Figure 1. Schematic geometry of the electric field-induced precessional magnetization switching. θ and φ are the direction angles describing the orientation of the macro-spin moment \mathbf{M} of free layer in spherical coordinates. The in-plane coercive field \mathbf{H}_c is parallel to the x axis. The external field \mathbf{H}_{ext} is applied along the positive direction of z axis. (a) and (b) are the calculated trajectories based on zero temperature LLG equation. $\mathbf{M}_{initial}$ and \mathbf{M}_{final} denote the initial and final magnetization state before and after voltage pulse duration τ_{pulse} . Blue line represents the precession process during τ_{pulse} , and red line represents the relaxation process after τ_{pulse} .

Before the voltage pulse is applied, the initial magnetization state $\mathbf{M}_{initial}$ is along the direction of effect field $\mathbf{H}_{eff}=\mathbf{H}_c+\mathbf{H}_{perp}+\mathbf{H}_{ext}$, where \mathbf{H}_{perp} is the out-of-plane anisotropy field. When apply a voltage pulse, a decrease of H_{perp} is induced by the electrical field modulation

[13], this will produce a net magnetic field H in the z positive direction:

$$H = H_{\text{ext}} - H'_{\text{perp}} \cos \theta, \quad (1)$$

where θ is the precession angle, H'_{perp} is the magnitude of out-of-plane anisotropy field when the voltage pulse is applied. Magnetization precession will take place under this induced net magnetic field.

Due to the non-zero in-plane coercive field \mathbf{H}_c , the precession axis tilts from the z axis. During the precession process, the \mathbf{H}_c changes from H_c to $-H_c$, the direction of precession axis will move, the precession angle θ will decrease in the first quarter of precession period and then increase in the later quarter of period. In this process, the precession angle θ also decreases gradually due to the damping effect. This will produce a net magnetic field H' in the z negative direction after τ_{pulse} :

$$H' = H_{\text{perp}} \cos(\theta_0 - \Delta\theta) - H_{\text{ext}} \approx H_{\text{perp}} [\cos(\theta_0 - \Delta\theta) - \cos \theta_0], \quad (2)$$

where θ_0 is the precession angle at initial equilibrium position and $\Delta\theta$ is the deviation of precession angle from its equilibrium position after τ_{pulse} . The net magnetic field H' will lead to a reversed magnetization precession. It is an increasing function with respect to $\Delta\theta$. When turn off the voltage pulse after the duration time nearby half precession period, if the $\Delta\theta$ is not large, under the effect of \mathbf{H}' and in-plane coercive field \mathbf{H}_c , the magnetization will swing around the equilibrium position and the final magnetization state will be stabilized to the reversed orientation with respect to the initial state during the relaxation process, as shown in figure 1(a). Therefore, a coherent magnetization switching can be realized by a unipolar voltage pulse. If the $\Delta\theta$ is large enough, the reversed precession will make the final magnetization state back to its initial orientation during the relaxation process, as shown in figure 2(b), so a switching error takes place.

To calculate the magnetization switching probability, we need to know the magnetization probability density distribution $P(\theta, \varphi)$ after the switching process. The switching process consists of the precession process during τ_{pulse} and the relaxation process after τ_{pulse} . The time-dependent $P(\theta, \varphi, t)$ follows the Fokker-Planck equation [21]:

$$\frac{\partial P}{\partial t} = \frac{1}{\sin \theta} \frac{\partial}{\partial \theta} \left\{ \sin \theta \left[\left(h \frac{\partial V}{\partial \theta} - g \frac{1}{\sin \theta} \frac{\partial V}{\partial \varphi} \right) P + k \frac{\partial P}{\partial \theta} \right] \right\} + \frac{1}{\sin \theta} \frac{\partial}{\partial \varphi} \left\{ \left(g \frac{\partial V}{\partial \theta} + h \frac{1}{\sin \theta} \frac{\partial V}{\partial \varphi} \right) P + k \frac{1}{\sin \theta} \frac{\partial P}{\partial \varphi} \right\}, \quad (3)$$

where $h = \frac{\alpha \gamma}{M_s + M_s \alpha^2}$, $g = -\frac{\gamma}{M_s + M_s \alpha^2}$, $k = k_B T h / v$, α is the damping factor, γ is the gyromagnetic

ratio, k_B is the Boltzmann constant, T is the temperature, M_s is the saturation magnetization, v is the volume of free layer and V is the effective potential energy under effect field \mathbf{H}_{eff} . V is given by: $V = -\mathbf{M} \cdot \mathbf{H}_{\text{eff}} = (-H_{\text{perp}}M_s \cos^2 \theta/2 - H_{\text{ext}}M_s \cos \theta - H_c M_s \sin^2 \theta \cos^2 \varphi/2)v$. The initial probability density distribution $P(\theta, \varphi, 0)$ is in its thermal equilibrium state, i.e., for $-\pi/2 \leq \varphi \leq \pi/2$, $P(\theta, \varphi, 0)$ is given by the Boltzmann distribution $P_0 \exp(-V/k_B T)$, and for $\pi/2 < \varphi < 3\pi/2$, $P(\theta, \varphi, 0) = 0$, where P_0 is the normalization constant: $P_0 = 1/\int_0^\pi d\theta \int_{-\pi/2}^{\pi/2} M_s^2 \sin \theta \exp(-V/k_B T) d\varphi$. Then the problem addressed is solving the partial differential equation (3). Once the probability density distribution $P(\theta, \varphi)$ after the switching process is obtained, the switching probability P_{switch} can be obtained by integral:

$$P_{\text{switch}} = \int_0^\pi d\theta \int_{\pi/2}^{3\pi/2} M_s^2 \sin \theta P(\theta, \varphi) d\varphi. \quad (4)$$

Then the error rate is obtained by $1 - P_{\text{switch}}$.

The Fokker-Planck equation (3) can be reduced to the standard eigenvalue problem by the method of separation of variables, which has been extensively studied involves the problems about relaxation time of a nanomagnet or the switching speed of thermally assisted spin torque-induced switching for $\Delta V/k_B T \gg 1$ [21-27], where ΔV is the energy barrier height between the bistable states. In this paper, the problem we care about is the probability density distribution evolution with respect to time. By moving and merging terms, (3) can be made of the form of an unsteady convection-diffusion equation:

$$\frac{\partial P}{\partial t} = a \frac{\partial^2 P}{\partial \theta^2} + b \frac{\partial P}{\partial \theta} + c \frac{\partial^2 P}{\partial \varphi^2} + d \frac{\partial P}{\partial \varphi} + eP, \quad (5)$$

where a, b, c, d, e are the coefficients of each term. The partial differential equation with the form of (5) can be solved numerically by the finite difference method directly. Using fourth order central difference scheme $\frac{1}{h}(-\frac{1}{12}P_{i+2} + \frac{2}{3}P_{i+1} - \frac{2}{3}P_{i-1} + \frac{1}{12}P_{i-2})$ for the first derivative with respect to θ and φ , and fourth order central difference scheme $\frac{1}{h^2}(-\frac{1}{12}P_{i+2} + \frac{4}{3}P_{i+1} - \frac{5}{2}P_i + \frac{4}{3}P_{i-1} - \frac{1}{12}P_{i-2})$ for the second derivative with respect to θ and φ , where h is the step of spatial coordinates, we constructed a difference scheme of Crank-Nicolson type with fourth order accuracy in space and second order accuracy in time to solve the partial differential equation (5). We used 400 meshes to sample the φ interval $(0, 2\pi)$ and 200 meshes to sample the θ range around the precession angle due to the small precession

angle change during the switching process. The time step was set as 0.2 ps. These values were carefully tested to ensure sufficient calculation accuracy.

3. Results and discussion

We adopted the values given in [13] for parameters used in the calculations. These values are listed as follows: The damping factor α is 0.01, the saturation magnetization M_s is 1.23×10^3 emu/cm³, the temperature T is 300 K, the volume v is 1.12×10^{-16} cm³, the in-plane coercive field H_c is 25 Oe, the perpendicular anisotropy field H_{perp} is 1400 Oe under zero bias voltage and 600 Oe under the applied voltage pulse. The calculated probability density distribution of the initial state and after a half-period τ_{pulse} of 0.46 ns under external field $H_{\text{ext}}=700$ Oe are shown in figure 2(a) and figure 2(b), respectively. It can be seen that the hot spot of probability density locates around (1.06, 0) at first and then moves to the position around (1.03, π), which indicates a 180 °magnetization reversal after the half-period pulse duration.

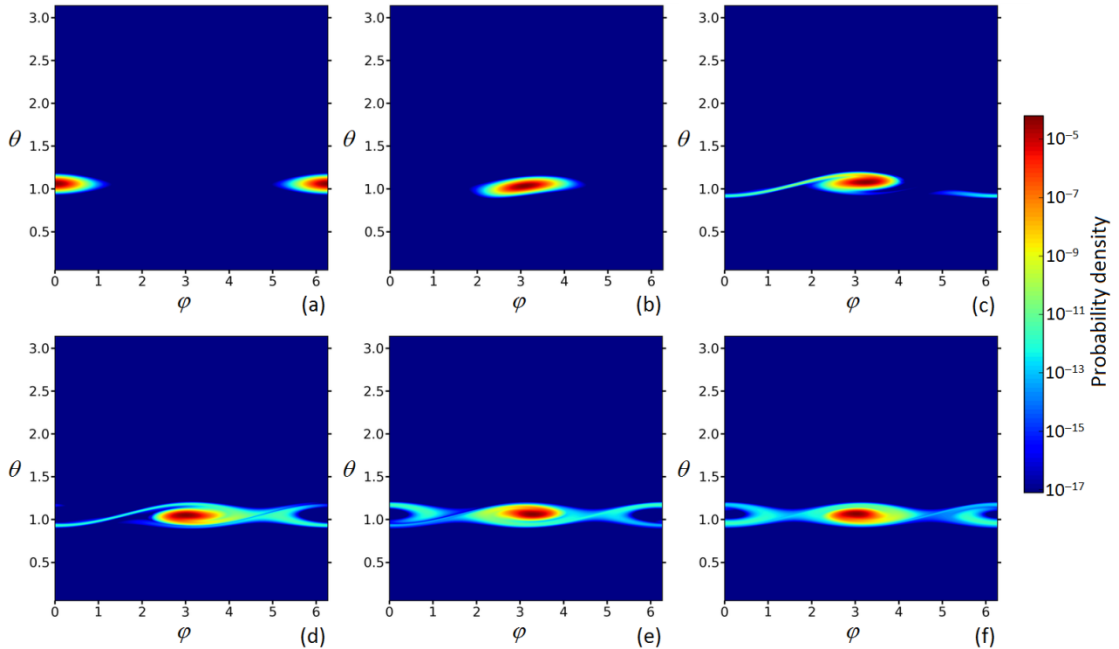


Figure 2. The calculated magnetization probability density distribution of (a): the initial state and (b): after half-period pulse duration of 0.46 ns under $H_{\text{ext}}=700$ Oe. The hot spot of probability density locates around (1.06, 0) at first and then moves to the position around (1.03, π), which indicates a 180 °magnetization reversal after the half-period pulse duration. (c)-(f): Evolution of the probability density distribution with relaxation time after the half-period pulse duration. (c): 1.25 ns; (d): 2.5 ns; (e): 3.75 ns; (f): 5 ns.

From figure 2(b), we can see the probability density distribution incline to the magnetization direction with large $\Delta\theta$ after the precession process. According to the discussion in section 2, this will cause reversed magnetization precession during the relaxation process, and cause switching error. We calculated the evolution of probability density distribution with time during the relaxation process after the half-period τ_{pulse} , as shown in figure 2(c)-(f). The relaxation time is (c) 1.25 ns, (d) 2.5 ns, (e) 3.75 ns and (f) 5 ns, respectively. It can be seen that a portion of probability density flows back to the interval $-\pi/2 \leq \varphi \leq \pi/2$ during the relaxation process, and tends to stabilized gradually with the increase of relaxation time. Using (4), we calculated the error rate as function of the relaxation time, as shown in figure 3(a). It can be seen that the error rate increases up to 1.5 ns and changes little

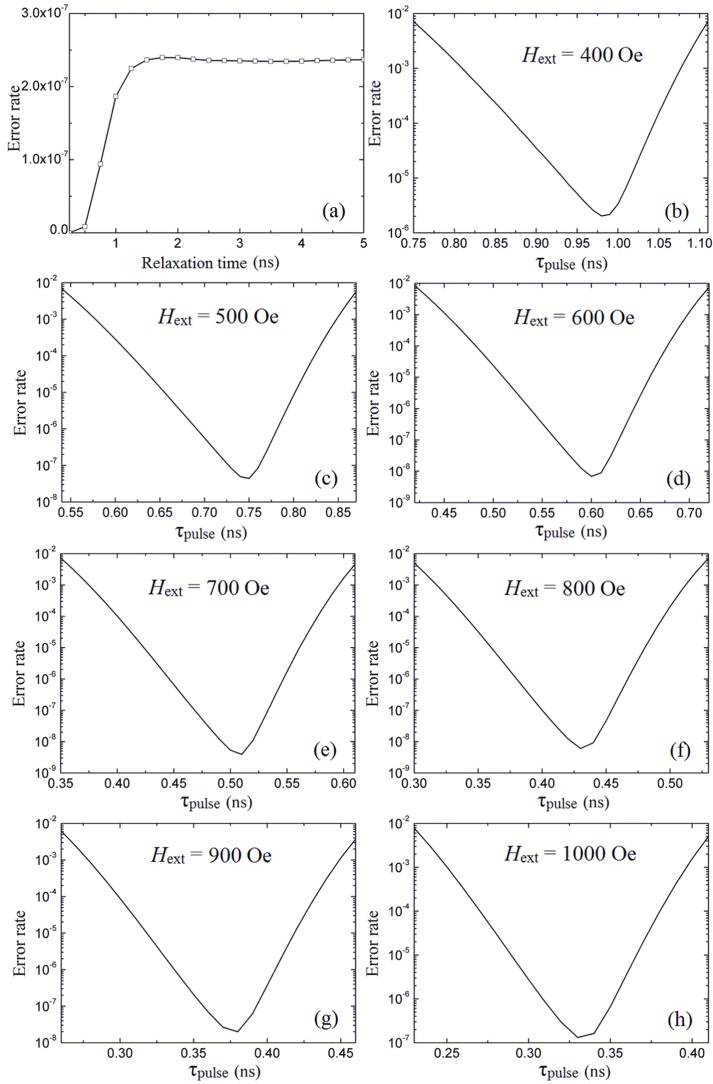


Figure 3. (a): The calculated error rate as function of relaxation time after 0.46 ns voltage pulse

duration under H_{ext} of 700 Oe. (b)-(h): The calculated error rate as function of pulse duration time τ_{pulse} for varied applied external field H_{ext} .

afterward. In the calculations below, the switching probability is obtained by integrating probability density distribution $P(\theta, \varphi)$ after sufficient relaxation time to ensure the calculation accuracy.

Figure 3(b)-(h) show the calculated error rate as function of pulse duration time τ_{pulse} for varied applied external field H_{ext} . All τ_{pulse} ranges are in the vicinity of the half precession period for the applied H_{ext} . The precession period is given by $2\pi(1+\alpha^2)/\gamma H$. Ignoring the change of precession angle θ during magnetization reversal, the estimated half-period time for H_{ext} of 700 Oe is about 0.46 ns. From figure 3(e) for $H_{\text{ext}}=700$ Oe, it can be seen that the τ_{pulse} with the lowest error rate is 0.51 ns. The τ_{pulse} with the lowest error rate is a little longer than the half-period time of the magnetization precession. This is a general result for varied H_{ext} . According to the discussion in section 2, due to the precession axis move during magnetization reversal, the precession angle θ will decrease first and then increase, so the $\Delta\theta$ has its smallest value at $\varphi=\pi$. Therefore, the τ_{pulse} with the lowest error rate is nearby the half-period time.

From figure 3, we can see ultra-low error rate less than 4×10^{-9} is achieved for $H_{\text{ext}}=700$ Oe. For the H_{ext} higher than 700 Oe, the error rate increases with the increase of H_{ext} , and for the H_{ext} lower than 700 Oe, the error rate increases with the decrease of H_{ext} . In the rest of this section, we discussed the influence of thermal stability factor, damping factor of free layer and spin transfer torque effect on the switching probability.

3.1. Influence of thermal stability

The thermal stability factor Δ of the free layer is estimated by $\Delta V/k_B T$, where ΔV is the anisotropy energy barrier height between the bistable states. Δ determines the initial magnetization probability density distribution before the applied voltage pulse. For the H_{ext} of 700 Oe and H_c of 25 Oe, the estimated Δ using the parameter values listed in section 3 is about 35. By increasing the H_c from 25 Oe to 36 Oe, a Δ value of 50 can be achieved. We calculated the error rate as function of τ_{pulse} for $\Delta=50$ under the H_{ext} of 700 Oe, as shown in

figure 4(a). The calculated results show that ultra-low error rate down to 5×10^{-12} is obtained for $\Delta=50$, the switching probability can be greatly improved by enhancing the thermal stability. For large Δ value, the initial probability density distribution concentrates to the equilibrium position with the lowest potential energy. Therefore, after the precession process, the probability density of magnetization direction with large $\Delta\theta$ decreases compared with the low Δ value, this leads to the decrease of switching error with the increase of Δ . This result suggests high-reliability write operations can be realized by electric field-induced precessional magnetization switching.

From figure 3 we can see that the error rate increases with the increase of H_{ext} in the high H_{ext} region. The increase of H_{ext} will cause large tilt of magnetization orientation, as shown in figure 1. This decreases the ΔV and leads to the decrease of thermal stability factor Δ . So the switching probability decreases for H_{ext} higher than 700 Oe.

Then we investigated the temperature dependence of the error rate, which is important for the high-reliability application. In Fokker-Planck equation (3), the thermal agitation term $k=k_{\text{B}}Th/\nu$ is proportional to the temperature T . The change of temperature not only influences the initial probability density distribution, but also influences the distribution during the magnetization precession process. The calculated results for $\Delta=35$ and $H_{\text{ext}}=700$ Oe are shown in figure 4(b), it can be seen that the error rate rises by about two orders of magnitude when the temperature rises from 300 K to 400 K. This indicates that the ambient temperature influence on the switching probability can't be ignored.

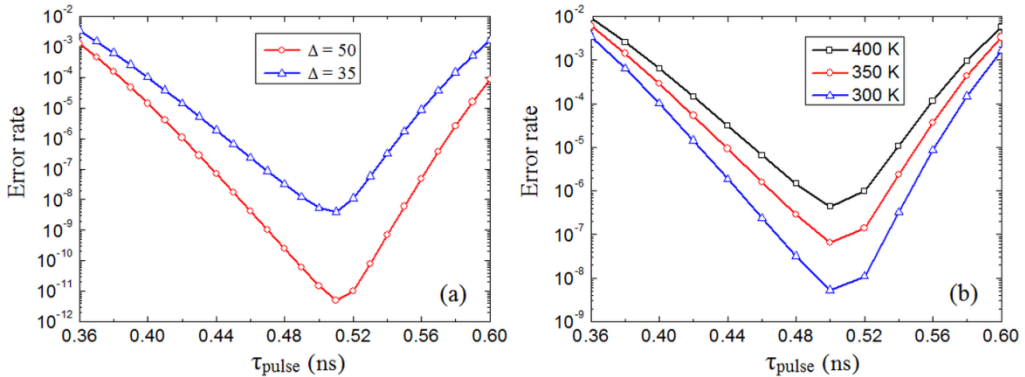


Figure 4. (a) The calculated error rate as function of pulse duration time τ_{pulse} under external field of 700 Oe. Red circle line: thermal stability factor Δ is 50; Blue triangle line: Δ is 35. (b) The calculated error rate as function of τ_{pulse} for external field of 700 Oe and Δ of 35 for different temperature. Black square line: 400 K; Red circle line: 350 K; Blue triangle line: 300 K.

3.2. Influence of damping factor α

During the magnetization precession process, the precession angle θ is the function of time t :

$$\tan \frac{\theta}{2} = e^{-\omega_0 t \alpha / (1 + \alpha^2)} \tan \frac{\theta_0}{2}, \quad (6)$$

where ω_0 is the precession angular frequency given by γH . Using (6), we can deduce:

$$\tan \frac{\Delta\theta}{2} = \tan \left(\frac{\theta_0}{2} - \frac{\theta}{2} \right) = \left(1 - e^{-\omega_0 t / (\alpha + \alpha^2)} \right) / \left(\frac{1}{\tan \frac{\theta_0}{2}} + e^{-\omega_0 t / (\alpha + \alpha^2)} \tan \frac{\theta_0}{2} \right). \quad (7)$$

From (7) it can be seen that $\Delta\theta$ is an increasing function with respect to α and θ_0 for $\alpha < 1$ and $\theta_0 < \pi/2$. From (2) we can see H' is also an increasing function with respect to θ_0 and $\Delta\theta$ for $\theta_0 < \pi/2$. Therefore, according to (2) and (7), the induced net magnetic field H' after τ_{pulse} increases with the increase of initial precession angle θ_0 .

From figure 3 it can be seen that the error rate increases with the decrease of H_{ext} in the low H_{ext} region. The decrease of H_{ext} will increase the tilt of precession axis from z axis, according to the discussion in section 2, this will increase $\Delta\theta$ after τ_{pulse} . The decrease of H_{ext} will also increase the initial precession angle θ_0 , and then increase the H' after τ_{pulse} . Therefore, the decrease of H_{ext} will cause more switching errors. Combining the influence of thermal stability in high H_{ext} region, the error rate will have the lowest value under an appropriate applied external field H_{ext} , here is the 700 Oe.

Increasing H_{ext} can decrease H' but it also decrease the thermal stability factor Δ and the magnetoresistance ratio due to the large magnetization tilt angle. According to (2) and (7), H' decreases with the decrease of damping factor α . In Fokker-Planck equation (3), the thermal agitation term $k = k_B T h / v$ is proportional to h , which also decreases with the decrease of α for $\alpha < 1$. Therefore, to improve the switching probability, we can employ low damping factor α material for the free layer. We calculated the error rate as function of τ_{pulse} for $\alpha = 0.005$ and 0.02 under the H_{ext} of 700 Oe, as shown in figure 5. It can be seen that ultra-low error rate can be achieved for the low α value, and for $\alpha = 0.02$, the error rate rises to the order of 10^{-5} . It also can be seen that τ_{pulse} with the lowest error rate is close to the half-period time with the decrease of α . These results suggest low damping factor material should be used for the free layer of the electric field-induced precessional magnetization switching.

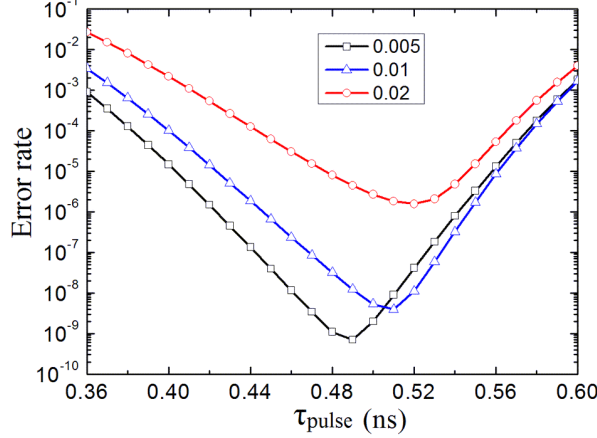


Figure 5. The calculated error rate as function of pulse duration time τ_{pulse} for different value of damping factor α under external field of 700 Oe. Black square line: $\alpha=0.005$; Blue triangle line: $\alpha=0.01$; Red circle line: $\alpha=0.02$.

3.3. Effect of spin transfer torque

Finally, we investigated the influence of spin transfer effect on the electric field-induced precessional magnetization switching. In [13], the current density passing through the device when voltage pulse is applied is $2.4 \times 10^6 \text{ A/cm}^2$, the torque introduced by the voltage is approximately 68 times that of spin transfer. Though the torque introduced by voltage dominates the precession process, the influence of spin transfer torque (STT) on the switching probability can't be neglected. We added the STT term $-\mathbf{M} \times (\mathbf{M} \times \mathbf{H}_s)$ [28] to the Fokker-Planck equation (3), where $\mathbf{H}_s = \left(\frac{J \hbar P}{2etM_s} \right) \mathbf{m}_s$, $J (2.4 \times 10^6 \text{ A/cm}^2)$ is the current density, $P (0.07)$ is the spin transfer coefficient, e is the electron charge, $t (0.7 \times 10^{-7} \text{ cm})$ is the free layer thickness, and \mathbf{m}_s is the unit magnetization vector of the pinned layer, the values in parentheses are from [13].

The calculated results for switching events from parallel (P) to anti-parallel (AP) magnetization configuration and from AP to P magnetization configuration are shown in figure 6(a). It can be seen that the STT effect influences the switching probability remarkably. To explain this, we analyze the dynamic process of magnetization precession. When an external magnetic field is applied, the magnetization vector \mathbf{M} tilts from $x-y$ plane to z axis, as shown in figure 1. The spin torque term $-\mathbf{M} \times (\mathbf{M} \times \mathbf{H}_s)$ will produce a net torque in the z direction. For P to AP, when $-\pi/2 < \varphi < \pi/2$ the z component of the torque is negative and will

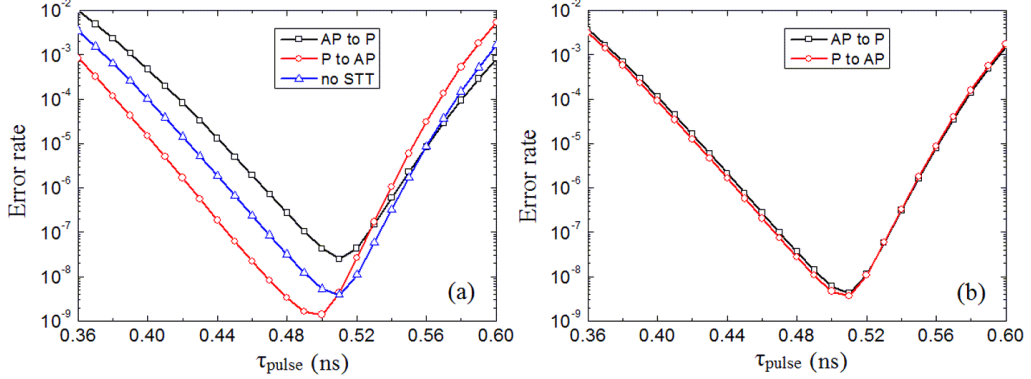


Figure 6. The calculated error rate as function of pulse duration time τ_{pulse} taking into account the spin transfer torque (STT) effect for the applied current density of (a) $2.4 \times 10^6 \text{ A/cm}^2$ and (b) $2.4 \times 10^5 \text{ A/cm}^2$, respectively. The external field H_{ext} is 700 Oe. Black square line: switching event from anti-parallel (AP) to parallel (P) magnetization configuration; Red circle line: switching event from P to AP; Blue triangle line: no STT effect is taken into account.

decrease the precession angle θ , when $\pi/2 < \varphi < 3\pi/2$ the z component is positive and will increase θ . If the z component of spin torque is not too large, it will decrease the $\Delta\theta$ when $\varphi < \pi$ and increase $\Delta\theta$ when $\varphi > \pi$, as shown in figure 7(a). This tends to decrease the error rate

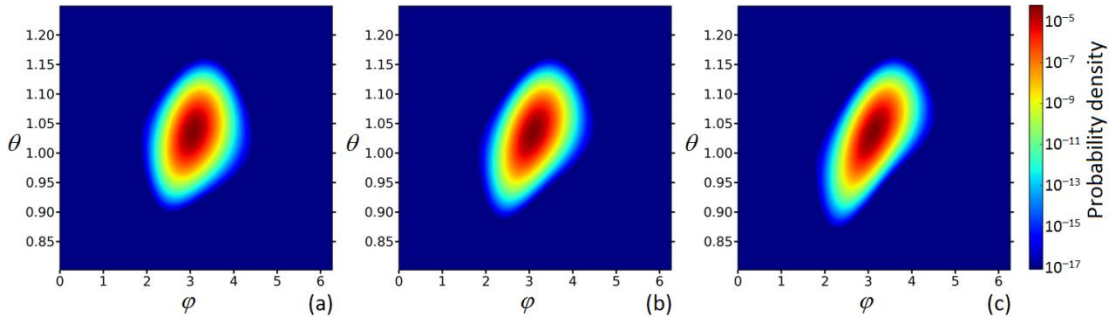


Figure 7. The calculated magnetization probability density distribution after 0.46 ns τ_{pulse} under the external field H_{ext} of 700 Oe. (a): the switching event from parallel (P) to anti-parallel (AP); (b): no STT effect is taken into account; (c): the switching event from AP to P.

when τ_{pulse} is shorter than the half-period, and increase the error rate when τ_{pulse} is longer than the half-period, as shown in figure 6(a). For AP to P, the situation is just the opposite, the z component of spin torque will increase the $\Delta\theta$ when $\varphi < \pi$ and decrease $\Delta\theta$ when $\varphi > \pi$, as shown in figure 7(c). Therefore, the error rate tends to increase when τ_{pulse} is shorter than the half-period and decrease when τ_{pulse} is longer than the half-period. We also calculated the error

rate for $J=2.4\times10^5$ A/cm², as shown in figure 6(b). It can be seen that the influence of STT effect on the switching probability can be ignored when the current density decreases by an order of magnitude [15].

4. Conclusions

In summary, we investigated the switching probability of electric field-induced precessional magnetization switching with in-plane easy axis by solving the Fokker-Planck equation numerically with finite difference method. The switching probability is determined by the net magnetic field H' induced by the deviation of precession angle θ from its equilibrium position after precession process. The error rate has the lowest value under an appropriate applied external field H_{ext} for the voltage pulse duration τ_{pulse} a little longer than the half precession period. The calculated results show that ultra-low error rate down to the order of 10^{-12} can be achieved for thermal stability factor $\Delta = 50$ and low damping factor material should be used for free layer to improve the switching probability. For parallel (anti-parallel) magnetization to anti-parallel (parallel) magnetization switching process, the spin transfer torque tends to decrease (increase) the error rate when the τ_{pulse} is shorter than the half precession period, and increase (decrease) the error rate when τ_{pulse} is longer than the half-period due to the z direction component of the torque. These results exhibit potential of the electric field-induced precessional magnetization switching for ultra-low power, high speed magnetic random access memory (MRAM) application. We hope this study is helpful to design the electric field-induced precessional magnetization switching device.

Acknowledgments

This work was supported by Tsinghua University Initiative Scientific Research Program (No. 20101081760) and Major State Basic Research Development Program 973 (No. 20101972110).

References

- [1] Weisheit M, Fähler S, Marty A, Souche Y, Poinsignon C and Givord D 2007 *Science* **315** 349
- [2] Duan C -G, Velev J P, Sabirianov R F, Zhu Z, Chu J, Jaswal S S and Tsymbal E Y 2008 *Phys. Rev. Lett.* **101** 137201
- [3] Maruyama T, Shiota Y, Nozaki T, Ohta K, Toda N, Mizuguchi M, Tulapurkar A A, Shinjo T, Shiraishi M, Mizukami S, Ando Y and Suzuki Y 2009 *Nat. Nanotechnol.* **4** 158
- [4] Shiota Y, Maruyama T, Nozaki T, Shinjo T, Shiraishi M and Suzuki Y 2009 *Appl. Phys. Express* **2** 063001
- [5] Tsujikawa M and Oda T 2009 *Phys. Rev. Lett.* **102** 247203
- [6] Nakamura K, Shimabukuro R, Fujiwara Y, Akiyama T, Ito T and Freeman A J 2009 *Phys. Rev. Lett.* **102** 187201
- [7] Niranjan M K, Duan C -G, Jaswal S S and Tsymbal E Y 2010 *Appl. Phys. Lett.* **96** 222504
- [8] Endo M, Kanai S, Ikeda S, Matsukura F and Ohno H 2010 *Appl. Phys. Lett.* **96** 212503
- [9] Ha S -S, Kim N -H, Lee S, You C -Y, Shiota Y, Maruyama T, Nozaki T and Suzuki Y 2010 *Appl. Phys. Lett.* **96** 142512
- [10] Nozaki T, Shiota Y, Shiraishi M, Shinjo T and Suzuki Y 2010 *Appl. Phys. Lett.* **96** 022506
- [11] Nozaki T, Shiota Y, Miwa S, Murakami S, Bonell F, Ishibashi S, Kubota H, Yakushiji K, Saruya T, Fukushima A, Yuasa S, Shinjo T and Suzuki Y 2012 *Nat. Phys.* **8** 491
- [12] Zhu J, Katine J A, Rowlands G E, Chen Y -J, Duan Z, Alzate J G, Upadhyaya P, Langer J, Amiri P K, Wang K L and Krivorotov I N 2012 *Phys. Rev. Lett.* **108** 197203
- [13] Shiota Y, Nozaki T, Bonell F, Murakami S, Shinjo T and Suzuki Y 2012 *Nat. Mater.* **11** 39
- [14] Kanai S, Yamanouchi M, Ikeda S, Nakatani Y, Matsukura F and Ohno H 2012 *Appl. Phys. Lett.* **101** 122403
- [15] Shiota Y, Miwa S, Nozaki T, Bonell F, Mizuochi N, Shinjo T, Kubota H, Yuasa S and Suzuki Y 2012 *Appl. Phys. Lett.* **101** 102406
- [16] Kanai S, Nakatani Y, Yamanouchi M, Ikeda S, Matsukura F and Ohno H 2013 *Appl. Phys. Lett.* **103** 072408

- [17] Parkin S S P, Kaiser C, Panchula A, Rice P M, Hughes B, Samant M and Yang S 2004 *Nat. Mater.* **3** 862
- [18] Yuasa S, Nagahama T, Fukushima A, Suzuki Y and Ando K 2004 *Nat. Mater.* **3** 868
- [19] Wang Z, Zhou Y, Zhang J and Huai Y 2012 *Appl. Phys. Lett.* **101** 142406
- [20] Nowak J J, Robertazzi R P, Sun J Z, Hu G, Abraham D W, Trouilloud P L, Brown S, Gaidis M C, O'Sullivan E J, Gallagher W J and Worledge D C 2011 *IEEE. Magn. Lett.* **2** 3000204
- [21] Brown Jr. W F 1963 *Phys. Rev.* **130** 1677
- [22] Aharoni A 1973 *Phys. Rev. B* **7** 1103
- [23] Coffey W T, Crothers D S F, Kalmykov Y P and Waldrom J T 1995 *Phys. Rev. B* **51** 15947
- [24] Koch R H, Katine J A and Sun J Z 2004 *Phys. Rev. Lett.* **92** 088302
- [25] Li Z and Zhang S 2004 *Phys. Rev. B* **69** 134416
- [26] Apalkov D M and Visscher P B 2005 *Phys. Rev. B* **72** 180405
- [27] He J, Sun J Z and Zhang S 2007 *J. Appl. Phys.* **101** 09A501
- [28] Xiao J, Zangwill A and Stiles M D 2004 *Phys. Rev. B* **70** 172405